Journal of the Serbian Chemical Society
JSCS-info@shd.org.rs • www.shd.org.rs/JSCS
J. Serb. Chem. Soc. 91 (0) 1–16 (2026)
JSCS–13530
Original scientific paper
Published 21 Aug 2026

Magnetic *Ambrosia artemisiifolia*-based biosorbent for Congo red removal from water: A circular economy approach

NATALIJA NEDIĆ[1], TAMARA TADIĆ[1], BOJANA MARKOVIĆ[1], ALEKSANDRA NASTASOVIĆ[1], ALEKSANDAR POPOVIĆ[2] and SANDRA BULATOVIĆ[1]*

[1]*Institute of Chemistry, Technology and Metallurgy, University of Belgrade, Njegoševa 12, 11000 Belgrade, Serbia and* [2]*University of Belgrade, Faculty of Chemistry, Studentski trg 12–16, 11158 Belgrade, Serbia*

(Received 9 September, revised 10 November, accepted 18 December 2025)

Abstract: Biomass-based biosorbents have demonstrated significant potential for removing synthetic organic dyes from water. This study explores the use of a magnetic biosorbent (Fe_3O_4/MB) derived from *Ambrosia artemisiifolia*, as a novel material for the removal of Congo red (CR) dye from aqueous solutions. The biosorption process was investigated by varying key parameters: pH, Fe_3O_4/MB dosage, CR concentration and temperature, followed by kinetic and equilibrium analyses. The structural properties of Fe_3O_4/MB were characterized using Fourier transform infrared spectroscopy. The CR concentration was monitored *via* UV–Vis spectrophotometry. Kinetic studies indicated that the biosorption of CR followed a PSO model (R^2 = 0.99). Isotherm analysis revealed that the Langmuir model best described the biosorption of CR (R^2 = 0.97), with a maximum adsorption capacity (Q_{max}) of 33.56 mg g^{-1}. The implementation of Fe_3O_4/MB supports sustainable water management and contributes to the development of greener and more circular industrial practices.

Keywords: biomass; biosorption; synthetic organic dyes; water treatment.

INTRODUCTION

Water pollution has become an escalating global problem. Synthetic organic dyes, used in the textile, paper and leather industries, significantly impact the environment and contribute to water contamination.[1] Many of these dyes are toxic, carcinogenic and resistant to degradation.[2] Reports indicate that about 700 tons of dye-laden industrial wastewater are released daily into the world's water bodies. Research reveals that even low concentrations of these compounds can be harmful to the environment.[3] Congo red (CR) is a widely used benzidine-based anionic azo dye, characterized by two azo groups, a long linear chain and two symmetrical

* Corresponding author. E-mail: sandra.bulatovic@ihtm.bg.ac.rs
https://doi.org/10.2298/JSC250909092N

naphthylamine moieties, with good water solubility and poor biodegradability. CR is primarily used in the textile and rubber industries and can enter the body through the skin, eyes, respiratory system or gastrointestinal tract, affecting vital organs and the immune system, including carcinogenic and mutagenic effects on human health.[4] Therefore, effectively removing CR from industrial wastewater is important for environmental protection.

Numerous techniques, such as adsorption, ozonation, advanced oxidation, reverse osmosis, flocculation, ion exchange, membrane separation, photocatalytic degradation and biodegradation, have been implemented to remove synthetic organic dyes from wastewater in order to reduce environmental pollution. Adsorption is the most widely used due to its operational simplicity, low cost, high efficiency and minimal sludge generation.[5,6] Various adsorbent materials, like synthetic polymers, nanocomposites, clays, modified adsorbents, carbon-based materials, *etc*., have been used for dye removal.[7] Among the many materials for dye sorption, biomass-based materials are an excellent choice because of their non-hazardous nature, wide availability in sufficient quantities, sorption efficiency and cost--effectiveness. These materials are not harmful to the environment and their use in environmental protection has become both an ecological and economic opportunity, representing an effective eco-friendly solution. Many researchers have investigated the use of biomass for wastewater treatment.[8–10] Biomass is composed of cellulose, lignin, hemicellulose, lipids and proteins, which contain functional groups (hydroxyl, carboxyl, amino and phenolic groups), making them effective for dye removal. A variety of biosorbents have been utilized in dye biosorption, such as microorganisms, agricultural wastes or weeds, forestry and food residues, wood wastes, *etc*.[11–13]

Ambrosia artemisiifolia is an invasive weed plant that has spread extensively across Europe, the Americas and Asia. In Europe alone, about 44 million people suffer from allergies caused by Ambrosia, resulting in high medical costs, with impaired quality of life for those patients. Beyond its allergenic effects, *A. artemisiifolia* can cause significant crop yield losses, exerting generally negative impacts on the environment.[14] This weed is particularly widespread in the northern regions of the Republic of Serbia, and the maximum recorded pollen concentration reached 12356 grains m^{-3}, making it the dominant airborne allergen.[15] Several researchers have explored the potential use of *A. artemisiifolia* as a biosorbent for removing some hazardous compounds, while its use in the removal of synthetic organic dyes remains largely unexplored.[16–18] Therefore, the literature on this topic remains limited, presenting opportunities for further investigation. In our previous study, a magnetic biosorbent derived from *A. artemisiifolia* biomass showed great potential for the removal of Malachite green (MG), a cationic dye, from aqueous

solutions.[19] The aim of this study was to examine the potential of the same magnetic biosorbent, Fe_3O_4/MB, for the sorption of a different type of dye, the anionic dye CR, while also considering a circular economy aspect of this research.

EXPERIMENTAL

Chemicals

The chemicals used in this research were: iron(II) chloride ($FeCl_2 \cdot 4H_2O$, ≥98 %), iron(III) chloride ($FeCl_3 \cdot 6H_2O$, ≥97 %), Congo red ($C_{32}H_{22}N_6Na_2O_6S_2$), sodium hydroxide (NaOH), sodium chloride (NaCl), acetone ($(CH_3)_2CO$), ethanol (C_2H_5OH), methanol (CH_3OH) and hydrochloric acid (HCl). All chemicals were purchased from Sigma–Aldrich.

Biosorbent material and characterization

The sample collection, biomass pre-treatment, preparation of magnetic biosorbent Fe_3O_4/MB, and its characterization (SEM, EDS, XRD and pH_{pzc}) were thoroughly described in detail in our previous paper.[19] The structure of Fe_3O_4/MB, before and after biosorption of CR dye, was characterized in this study using a Nicolet Summit FT-IR spectrometer (Thermo Fisher Scientific, Waltham, MA, USA), in ATR mode over the range 4000–400 cm^{-1}.

Biosorption study in a batch system

Determination of the optimal conditions for the efficient biosorption of CR with Fe_3O_4/MB in a batch system, was achieved by monitoring the effects of biosorbent dose (1–5 g L^{-1}), contact time (0–180 min), dye concentration (10–300 ppm), pH (2–10) and temperature (298––318 K). For monitoring the biosorption process, 5 g L^{-1} of Fe_3O_4/MB was added to a vial flask containing 20 mL of a 50 ppm CR solution, based on the experience from our previous study.[19] The samples were shaken for 180 min at 450 rpm, in an orbital shaker (Orb-Pro Labbox Labware, Barcelona, Spain). After the biosorption process, the Fe_3O_4/MB was separated using an external magnet and the remaining CR concentration was measured using a UV–Vis spectrophotometer, at λ_{max} = 498 nm. UV–Vis spectroscopy (Novel-102S, COLOLab Experts, Polje ob Sotli, Slovenia) was used for determining the CR concentrations. The removal efficiency (R in %), and the biosorption capacity (Q_t, in mg g^{-1}) of CR were calculated as:[20]

$$R = 100\frac{c_0 - c_e}{c_0} \tag{1}$$

$$Q_t = \frac{(c_0 - c_t)V}{m} \tag{2}$$

where c_0, c_e and c_t (ppm) represent the CR concentrations in the aqueous solution at the initial, equilibrium and any time t; V (L) is the water solution volume; m (g) is the biosorbent mass.

For the desorption experiment Fe_3O_4/MB (5 g L^{-1}) was added to the CR dye solution (c_0 = 50 ppm; pH 3; T = 298 K; contact time = 180 min; shaking speed = 450 rpm). After CR biosorption, the CR-loaded Fe_3O_4/MB was separated using an external magnet. Desorption agents (20 mL), including absolute EtOH,[21] 0.1 M HCl,[21] 0.1 M NaOH,[21] distilled water,[22] acetone,[23] MeOH and 10 % NaCl:MeOH (volume ratio 3:7),[24] were used for desorption of CR from the CR-loaded Fe_3O_4/MB, and shaken for 60 min at 450 rpm. The samples were separated using an external magnet and the concentrations of CR were measured using a UV–Vis spectrophotometer at λ_{max} = 498 nm. The desorption percentage (D in %) of CR was determined using as:[25]

$$D = 100\frac{Q_d}{Q_a} \quad (3)$$

where Q_d and Q_a (mg g^{-1}) are the desorbed and adsorbed quantities of CR.

RESULTS AND DISCUSSION

FTIR characterization of Fe_3O_4/MB

The Fourier transform infrared spectroscopy (FTIR) spectrum of Fe_3O_4/MB, before and after biosorption of CR, given in Fig. 1, shows the presence of many functional groups responsible for dye biosorption. The broad band at 3331.8 cm^{-1} is characteristic of the stretching vibration of hydroxyl groups (–OH) and primary amines stretching (–NH), probably connected to hydrogen bonds within cellulose and lignin.[26,27] The peaks at 2919.1 and 2850.9 cm^{-1} can be attributed to C–H stretching vibrations in $–CH_2$ and –CH groups. The absorption peaks at 1641.5 and 1419.6 cm^{-1} indicate the presence of –COO of carboxyl and C–O groups on the Fe_3O_4/MB surface.[22,28] The peak at 1260.9 cm^{-1} can refer to stretching of the COC group, while the peak at 1026.5 cm^{-1} corresponds to the CO stretching vibration of primary alcohols. [29] The spectrum after CR biosorption didn't show significant changes in peaks intensities in the region from 3300–2000 cm^{-1}, but in the region from 2000–500 cm^{-1} changes in intensities and appearance of a new peaks at 1602.5, 1421.2, and 1041.1 cm^{-1} were evident, due to the dye biosorption on the Fe_3O_4MB surface.[30] The peak at 587.7 cm^{-1} is related to magnetite, incurporated into the structure of magnetic Fe_3O_4/MB.[31] According to these results, the functional groups potentially involved in the biosorption of CR dye include hydroxyl, carboxyl and amine groups. The shifting of peak frequency and intensity in the FTIR spectrum of CR-loaded Fe_3O_4/MB, compared to the Fe_3O_4/MB could be assigned to the biosorption of CR on the Fe_3O_4/MB surface. In general, the biosorption of CR with Fe_3O_4/MB occurs through hydrogen bonding, electrostatic

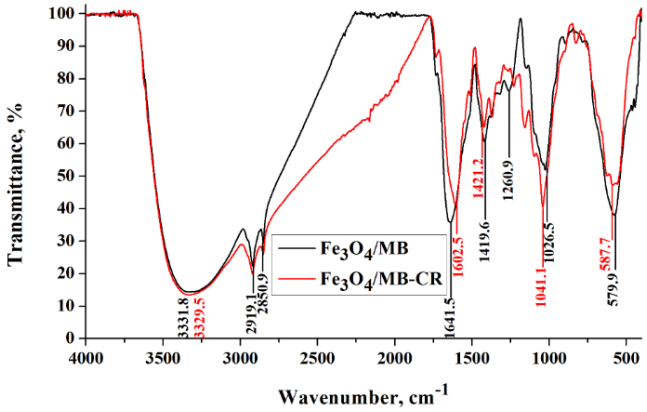

Fig. 1. FTIR spectra of Fe_3O_4/MB and Fe_3O_4/MB–CR.

interaction, π–π interactions and ion exchange. The presence of cellulose, hemicellulose and lignin in the biosorbent structure, with a large number of hydroxyl, carbonyl and carboxyl functional groups, allows CR biosorption from aqueous solutions.[27]

Effect of pH on biosorption

The pH of the CR solution plays a crucial role in determining the biosorption capacity, because it directly affects the surface charge of the Fe_3O_4/MB and the ionization of the CR. The removal efficiency of CR from aqueous solutions using Fe_3O_4/MB was evaluated across a range of pH values (2–10), while maintaining constant experimental conditions (c_0 = 50 ppm, Fe_3O_4/MB dose = 5 g L^{-1}, T = 298 K, contact time = 180 min and shaking speed = 450 rpm). The pH of the CR solutions was adjusted using a pH meter and by adding 0.1 M NaOH or 0.1 M HCl solutions. Fe_3O_4/MB was added to each solution, after which the samples were shaken. After the biosorption process at different pH, the samples were separated using an external magnet, and the concentrations of CR were measured using a UV–Vis spectrophotometer at λ_{max} = 498 nm. As illustrated in Fig. 2a, the CR removal percentage increased from 32.23 % at pH 10 to a maximum of 82.88 % at pH 3. At pH values below the point of zero charge (pH_{pzc} 4.8),[19] the Fe_3O_4/MB surface is positively charged, leading to electrostatic attraction between the Fe_3O_4//MB and the anionic CR dye, which increased biosorption efficiency (Fig. 3). In contrast, at pH values above 4.8, the Fe_3O_4/MB surface becomes negatively charged, leading to a decrease in CR biosorption.

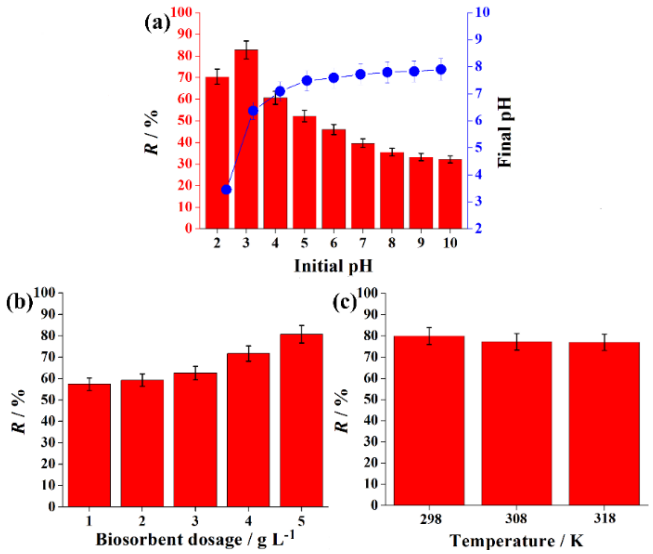

Fig. 2. The effects of the experimental parameters: a) initial pH (2–10) and final pH, b) Fe_3O_4/MB dose (1–5 g L^{-1}) and c) T (298–318 K), on CR biosorption onto Fe_3O_4/MB.

The pH analysis of CR solutions before and after biosorption of CR with Fe_3O_4/MB revealed a dependence on the initial acidity of the solution. Under acidic conditions, the final pH values increased relative to the initial pH, whereas in basic conditions, the pH remained largely unchanged, reaching a plateau. Notably, at the optimal pH 3, a pronounced change in pH was observed (from 3 to 6.37), corresponding to the highest CR removal. Hence, acidic conditions were more favorable for the biosorption process of CR onto Fe_3O_4/MB, which is in accordance with literature data.[32,33]

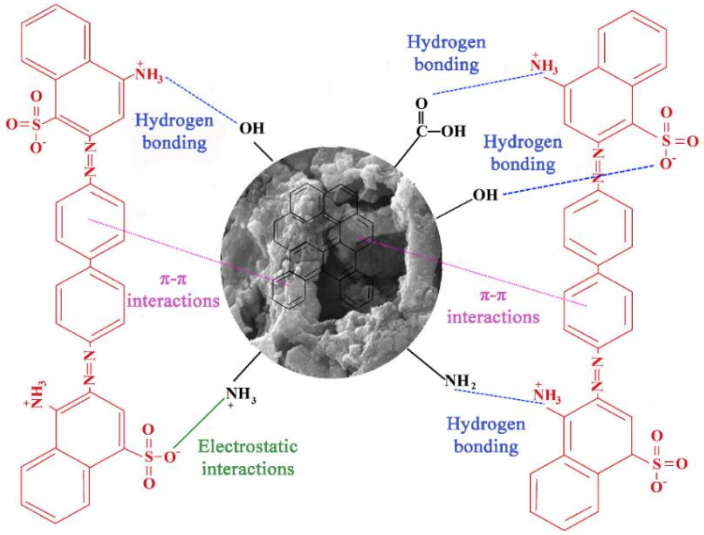

Fig. 3. Proposed biosorption mechanisms of CR biosorption onto Fe_3O_4/MB at pH 3.

Effect of biosorbent dose

The effect of varying Fe_3O_4/MB doses (1–5 g L^{-1}) on the removal efficiency of CR was investigated while keeping all other experimental parameters constant (c_0 = 50 ppm, pH 3, T = 298 K, contact time = 180 min, and shaking speed = 450 rpm). The results indicate that CR removal efficiency increased from 57.39 to 80.72 % as the Fe_3O_4/MB dose was raised from 1 to 5 g L^{-1} (Fig. 2b). This is attributed to the greater availability of active sites on the Fe_3O_4/MB surface at higher doses, which facilitates dye biosorption. Based on these results, an Fe_3O_4/MB dose of 5 g L^{-1} was selected as the optimal dose for CR removal.

Biosorption thermodynamics

The thermodynamic parameters – Gibbs energy ($\Delta G°$), enthalpy ($\Delta H°$) and entropy ($\Delta S°$) changes for the biosorption of CR onto Fe_3O_4/MB were evaluated at three different temperatures (298, 308 and 318 K), while maintaining constant

experimental conditions (c_0 = 50 ppm, Fe_3O_4/MB dose = 5 g L^{-1}, pH 3, contact time = 180 min, and shaking speed = 450 rpm). The reduction in CR uptake capacity of the Fe_3O_4/MB at higher temperatures might be due to the weakening of interactions between the dye molecules and the active sites on the Fe_3O_4/MB surface (Fig. 2c). The negative values of $\Delta G°$ (Table I), in the temperature range 298–318 K suggest that the biosorption of CR with Fe_3O_4/MB is spontaneous. The negative values of $\Delta H°$ and $\Delta S°$ (Table I) indicate the exothermic nature of the biosorption process, associated with decreased randomness and disorder at the solid–liquid interface.[34] The thermodynamic parameters were determined using the Van't Hoff Eqs.:[8,35]

$$\Delta G° = -RT \ln K_d \tag{4}$$

$$K_d = \frac{Q_e}{c_e} \tag{5}$$

$$\log K_d = \frac{\Delta S°}{2.303R} - \frac{\Delta H°}{2.303RT} \tag{6}$$

$$\Delta G° = \Delta H° - T\Delta S° \tag{7}$$

where R is the ideal gas constant (8.314 J mol^{-1} K^{-1}), T is the Kelvin temperature of biosorption, K_d is the linear sorption distribution coefficient, Q_e (mg g^{-1}) is the equilibrium adsorption capacity representing the mass of CR adsorbed per unit mass of the biosorbent and c_e (mg L^{-1}) is the equilibrium concentration of the dye in solution.

TABLE I. Thermodynamic parameters for the biosorption of CR onto Fe_3O_4/MB

$\Delta H°$ / kJ mol^{-1}	$\Delta S°$ / J mol^{-1} K^{-1}	$\Delta G°$ / kJ mol^{-1}		
		298 K	308 K	318 K
−6.97	−25	−0.56	−0.98	−1.06

Biosorption kinetics

The influence of contact time on the removal efficiency of CR by Fe_3O_4/MB is illustrated in Fig. 4. The biosorption process demonstrated a relatively rapid uptake, reaching ~83 % removal within 120 min. Initially, the biosorption rate was high due to the abundance of available binding sites on the Fe_3O_4/MB surface. Over time, the rate of CR biosorption decreased, suggesting saturation of the binding sites. For a better understanding of the biosorption mechanism, the experimental data were fitted to the linearized forms of four kinetic models: pseudo-first-order (PFO), pseudo-second-order (PSO), Elovich and intra-particle diffusion (IPD) model (Table S-I of the Supplementary material to this paper). According to the results (Table II; Fig. 5), the PSO model provided the best fit, with a correlation coefficient (R^2) of 0.99. Furthermore, the calculated equilibrium biosorption cap-

acity from the PSO model (8.68 mg g^{-1}) closely matched the experimentally determined value (Fig. 4; 8.36 mg g^{-1}), confirming the suitability of the PSO model for describing the biosorption kinetics of CR onto Fe_3O_4/MB.

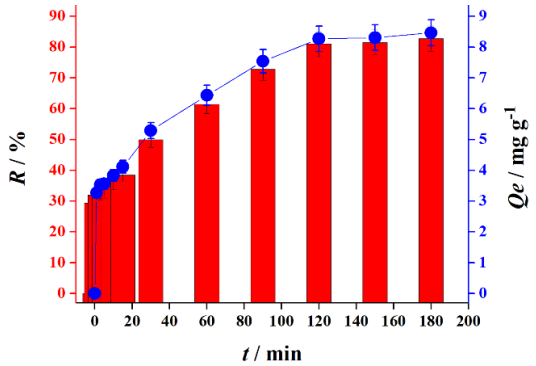

Fig. 4. Effect of contact time on the removal of CR onto Fe_3O_4/MB (c_0 = 50 ppm; Fe_3O_4/MB dose = 5 g L^{-1}; T = 298 K; pH 3; shaking speed = 450 rpm).

TABLE II. Kinetic parameters of various models for the biosorption of CR onto Fe_3O_4/MB

Parameter	Value
Q_e^{exp} / mg g^{-1}	8.36
PFO	
Q_e^{cal} / mg g^{-1}	5.83
k_1 / min^{-1}	0.02
R^2	0.97
PSO	
Q_e^{cal} / mg g^{-1}	8.68
k_2 / g mg^{-1} min^{-1}	0.01
R^2	0.99
Elovich model	
α_E / mg g^{-1}	7.20
β_E / g mg^{-1}	0.89
R^2	0.88
IPD model	
k_3 / g mg^{-1} min^{-1}	0.46
R^2	0.98

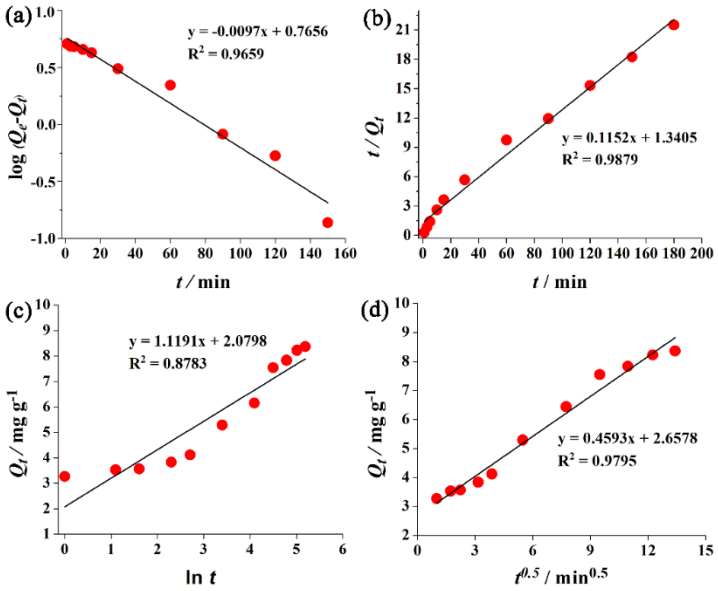

Fig. 5. Linear plots of kinetics models: (a) PFO, (b) PSO, (c) Elovich, and (d) IPD model, for the biosorption of CR onto Fe_3O_4/MB.

Biosorption isotherms

Fig. 6 illustrates the biosorption of CR onto Fe_3O_4/MB at varying initial dye concentrations (10–300 ppm), using a constant Fe_3O_4/MB dose of 5 g L^{-1}, with contact times ranging from 0 to 180 min, at 298 K and pH 3. The experiments were conducted under constant experimental conditions. The results demonstrate that increasing the initial CR concentration leads to an increase in the biosorption capacity of Fe_3O_4/MB. The experimental data were fitted to the Langmuir, Freundlich, Temkin, Elovich and Dubinin–Radushkevich isotherm models (Table S-II of the Supplementary material). The Langmuir model, which assumes monolayer adsorption on a homogeneous surface with uniform energy sites, showed the best fit, as indicated by a high coefficient of determination (R^2 = 0.97, Table III; Fig. 7). The theoretical maximum adsorption capacity calculated from the Langmuir model was 33.56 mg g^{-1}, which is close to the experimentally determined value of 29.64 mg g^{-1}. The Dubinin–Radushkevich model is important for determining of the adsorption energy (E) and underlying sorption mechanisms (physical or chemical), responsible for CR removal. The adsorption processes with E levels < 8 kJ mol^{-1} reflect physical, between 8 and 16 kJ mol^{-1} reflect combination of physical chemical and higher than 16 kJ mol^{-1} reflect chemical-based mechanisms.[36] The E values detected in this study > 8 kJ/mol (11.28 kJ mol^{-1}) aligns with the energies for cooperative processes involving physical and chemical interactions (8−16 kJ

mol^{-1}), indicating that ion exchange is the dominant process of absorption of CR onto Fe_3O_4/MB,[37] which is consistent with other results.

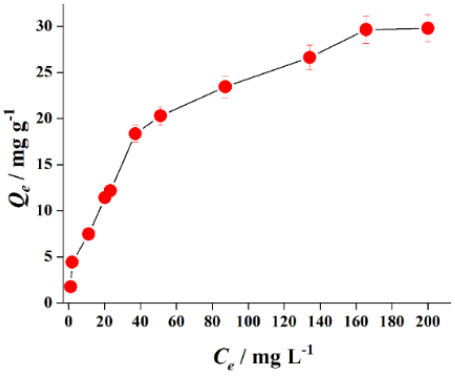

Fig. 6. Influence of the initial concentration of CR and contact time on the CR biosorption capacity onto Fe_3O_4/MB.

TABLE III. Parameters for various isotherm models of CR biosorption onto Fe_3O_4/MB

Parameter	Value
Langmuir model	
Q_m / mg g^{-1}	33.5
K_L / L mg^{-1}	0.03
R^2	0.97
Freundlich model	
n_F	1.89
K_F / L g^{-1}	2.26
R^2	0.96
Temkin model	
A_T / L mg^{-1}	0.73
R^2	0.91
Elovich model	
Q_m / mg g^{-1}	12.58
K_E / L g^{-1}	0.12
R^2	0.88
Dubinin–Radushkevich	
$K_{D\text{-}R}$ / mol^2 kJ^{-2}	3.93×10^{-6}
E / kJ mol^{-1}	11.28
$Q_{D\text{-}R}$ / mg g^{-1}	162.32
R^2	0.97

Comparison studies

The maximum biosorption capacity of Fe_3O_4/MB for CR was evaluated by comparison with other biosorbents reported in the literature (Table IV). Based on the Langmuir isotherm model, in this study, the calculated maximum capacity was 33.56 mg g^{-1}, indicating that Fe_3O_4/MB exhibits competitive efficiency and promising potential for application in the treatment of dye-contaminated wastewater.

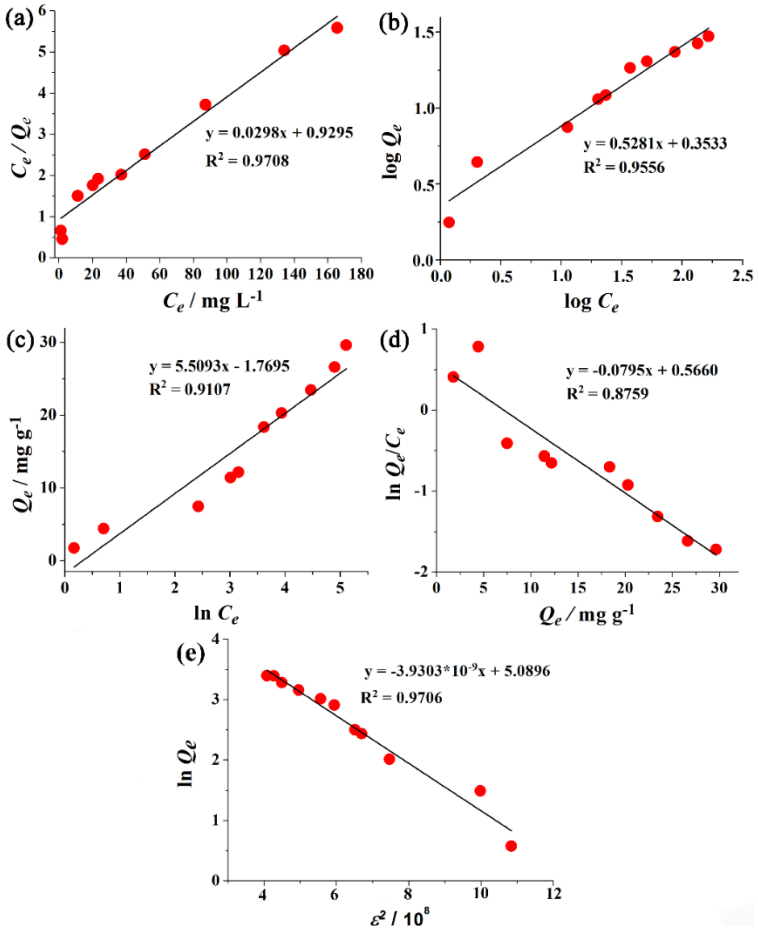

Fig. 7. Linear plots of isotherm models: a) Langmuir, b) Freundlich, c) Temkin, d) Elovich and e) Dubinin–Radushkevich model for the biosorption of CR onto Fe_3O_4/MB.

In addition to its notable performance, the application of Fe_3O_4/MB has several advantages: it is a minimally modified, inexpensive and readily available biomaterial, making it attractive for practical applications and contributing to the reduction of the harmful impact of weeds on the environment and human health. Moreover, this biosorbent has not been previously analysed for CR removal and, to date, no studies have reported its application for this purpose in the available literature. Although these results are favourable compared to many low-cost and biomass--based biosorbents, it is important to note that the referenced data were obtained under different experimental conditions. Variations in initial dye concentration, pH, biosorbent dosage, contact time and temperature can significantly influence

the results. Therefore, to enable a more accurate comparison, further studies under standardized conditions are recommended.

TABLE IV. Comparison of CR removal using different biosorbents

Biosorbent	Conc. ppm	pH	Biosorbent dose, g L^{-1}	Time min	Temp. K	Q_{max} mg g^{-1}	Ref.
Fe_3O_4/MB	50	3	5	180	298	33.50	–
Garlic peel	25	5	7	15	298	15.22	38
Oyster shells	72.34	3.3	0.1	84.44	298	84.77	3
Cotton calyx–Fe_3O_4	25	1–10	24	60	293	20.66	39
Vangueria infausta fruit pericarp	10	2	14	180	328	7.91	40
Pleurotus mutilus	50	3.5	1	150	300	36.68	41
Wood bimass	50	7	0.008	360	298	8.00	27
Modified egg shell membrane	100	4.5	10	180	298	117.65	42

Regeneration of Fe_3O_4/MB

A regeneration study of Fe_3O_4/MB was conducted using seven different desorption agents: 0.1 M HCl, 0.1 M NaOH, absolute EtOH, acetone, MeOH and 10 % NaCl:MeOH (volume ratio 3:7). The results, shown in Fig. 8a, indicate that 10 % NaCl:MeOH was the most effective desorbing agent after the first adsorption/desorption cycle, and it was used for all subsequent regeneration tests. As depicted in Fig. 8b, the desorption efficiency of CR decreased significantly from 98.32 to 46.0 % over five regeneration cycles. Several factors could explain the significant decline. Repeated exposure of the biosorbent to the CR likely causes physical or chemical degradation, which negatively impacts its performance across multiple adsorption/desorption cycles. Also, it is possible that the regeneration procedure used in this study isn't effective in achieving total removal of all CR molecules from the biosorbent surface, leading to fewer available active sites after each cycle. The Fe_3O_4/MB particles may have agglomerated during the biosorption process, reducing the overall biosorption capacity over time. To address these

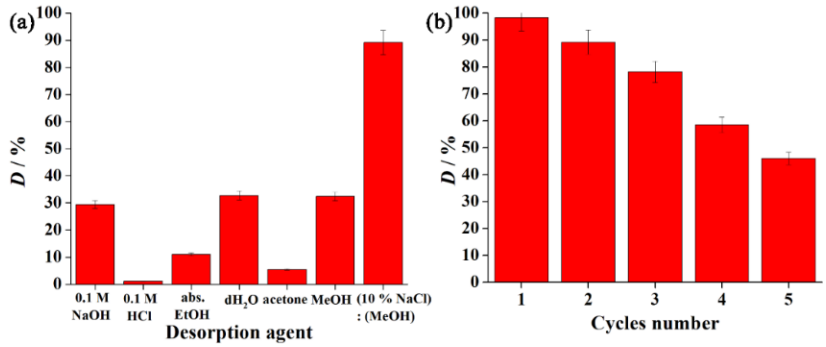

Fig. 8. A regeneration/reusability study of Fe_3O_4/MB: a) Examined CR desorption agents; b) number of CR desorption cycles.

challenges and improve the reusability of the Fe_3O_4/MB, it is essential to optimize the regeneration conditions. This involves identifying the ideal protocol that guarantees complete CR desorption while minimizing any possible interruption.[9]

Circular-economy approach

The circular economy is a production/consumption model that involves 4R's, including repairing, reusing, refurbishing and recycling of existing materials and bioproducts.[43] Adopting a circular economy approach in wastewater treatment emphasizes the reuse of natural, renewable resources to minimize waste and environmental impact. Utilizing biomass-based biosorbents such as Fe_3O_4/MB, which is derived from *A. artemisiifolia*, a widely distributed weed species whose collection incurs no cost, aligns with this strategy by transforming low-value plant material into an effective tool for pollutant removal. This not only reduces dependence on synthetic or energy-intensive adsorbents but also adds value to biological waste, thereby closing the loop between resource use and waste generation. Implementing such biosorption systems supports sustainable water management and contributes to the development of greener, more circular industrial practices.[44]

CONCLUSION

This study demonstrated the strong potential of Fe_3O_4/MB, derived from *Ambrosia artemisiifolia* biomass, for the biosorption of Congo red (CR) in a batch system. Kinetic analysis confirmed that the PSO model best describes the biosorption process of CR, indicating that chemisorption is the rate-limiting step. Isotherm analysis revealed that the Langmuir model accurately fit the experimental data, suggesting monolayer adsorption of CR on the biosorbent surface. Under optimal experimental conditions (c_0 = 50 ppm; Fe_3O_4/MB dose = 5 g L^{-1}; T = 298 K; t = 180 min; pH 3), the maximum CR adsorption capacity was 33.56 mg g^{-1}. These findings indicate that Fe_3O_4/MB is an economical, environmentally friendly and effective alternative for CR removal from wastewater.

Compared to our previous study, Fe_3O_4/MB proved to be effective for the sorption of anionic dyes, but with a slight advantage for cationic dyes, as the biosorption efficiency (91.81 % for MG; 83.68 % for CR) was higher at shorter sorption times (60 min for MG; 180 min for CR). Both studies observed that the dye uptake using the same biosorbent was best fit to the Langmuir isotherm and the PSO kinetic model. Thermodynamic modelling revealed that both biosorption processes were spontaneous and exothermic. In summary, we presume that the CR and MG uptakes by the Fe_3O_4/MB were achieved by a combination of electrostatic attraction, π–π electron–donor interaction and hydrogen bonds. Therefore, Fe_3O_4/MB could serve as an alternative adsorbent/biosorbent for the treatment of contaminated water that contains different synthetic organic dyes. Future research will explore Fe_3O_4/MB applicability for removing a broader range of contaminants

such as pesticides and pharmaceuticals, as well as scaling-up from laboratory to industrial applications. This will require a thorough assessment of technological feasibility and economic viability.

SUPPLEMENTARY MATERIAL

Additional data and information are available electronically at the pages of journal website: https://www.shd-pub.org.rs/index.php/JSCS/article/view/13530, or from the corresponding author on request. This work is related to the implementation of the United Nations Sustainable Development Goal 6 – Clean water and sanitation.

Acknowledgement. This research has been financially supported by the Ministry of Science, Technological Development and Innovation of Republic of Serbia (Contracts No. 451-03-136/2025-03/200026 and 451-03-136/2025-03/200168).

ИЗВОД

МАГНЕТИЧНИ БИОСОРБЕНТ НА БАЗИ БИОМАСЕ *Ambrosia artemisiifolia* ЗА УКЛАЊАЊЕ КОНГО ЦРВЕНЕ ИЗ ВОДЕ: ЦИРКУЛАРНО-ЕКОНОМСКИ ПРИСТУП

НАТАЛИЈА НЕДИЋ[1], ТАМАРА ТАДИЋ[1], БОЈАНА МАРКОВИЋ[1], АЛЕКСАНДРА НАСТАСОВИЋ[1], АЛЕКСАНДАР ПОПОВИЋ[2] и САНДРА БУЛАТОВИЋ[1]

[1]Институт за хемију, технологију и металургију Универзитет у Београду, Његошева 12, 11000 Београд и [2]Универзитет у Београду, Хемијски факултет, Студентски трг 12–16, 11158 Београд

Биосорбенти на бази биомасе показали су значајан потенцијал за уклањање синтетичких органских боја из воде. Ова студија заснива се на употреби магнетичног биосорбента (Fe_3O_4/MB) на бази биомасе *Ambrosia artemisiifolia*, као новог материјала за уклањање конго црвене (CR) боје из воденог раствора. Процес биосорпције је испитиван варирањем кључних параметара: pH, доза биосорбента, концентрација боје и температура, након чега су уследиле кинетичке и равнотежне анализе. Структурна својства Fe_3O_4/MB су окарактерисана Фуријеовом трансформационом инфрацрвеном спектроскопијом. Концентрација боје праћена је UV–Vis спектрофотометријом. Кинетичке анализе су показале да биосорпција боје прати PSO модел (R^2 = 0,99). Ленгмиров модел изотерми показао је најбоље слагање са експерименталних подацима (R^2 = 0,97), са максималним капацитетом адсорпције (Q_{max}) од 33,56 mg g^{-1}. Примена Fe_3O_4/MB подржава одрживо управљање водама и доприноси развоју еколошки прихватљивих и циркуларних индустријских пракси.

(Примљено 9. септембра, ревидирано 8. октобра, прихваћено 18. децембра 2025)

REFERENCES

1. S. He, J. Sun, X. Jin, Q. Chen, X. Wu, F. Tian, X. Zhang, P. Li, H. Sheng, *Diam. Relat. Mater.* **136** (2023) 109930 (https://doi.org/10.1016/j.diamond.2023.109930)
2. I. Muneer, T. Javed, A. A. Majeed, H. T. Masood, *Desalin. Water Treat.* **235** (2021) 272 (https://doi.org/10.5004/dwt.2021.27596)
3. A. O. Adeleke, R. C. Omar, K. K. Katibi, T. T. Dele-Afolabi, A. Ahmad, J. O. Quazim, A. A. Amusa, M. B. Alshammari, *Alex. Eng. J.* **92** (2024) 11 (https://doi.org/10.1016/j.aej.2024.02.042)

4. N. K. Soliman, M. Shaban, S. A. Ahmed, A. R. Dryaz, H. R. A. El-Mageed, R. El-Sayed, E. S. Allehyani, H. M. Al-Saidi, K. N. M. Elsayed, A. Hamd, *Desalin. Water Treat.* **267** (2022) 266 (https://doi.org/10.5004/dwt.2022.28688)
5. J. N. Wekoye, W. C. Wanyonyi, P. T. Wangila, M. K. Tonui, *Environ. Chem. Ecotoxicol.* **2** (2020) 24 (http://dx.doi.org/10.1016/j.enceco.2020.01.004)
6. A. N. Kani, E. Dovi, A. A. Aryee, F. M. Mpatani, R. Han, Z. Li, L. Qu, *Desalin. Water Treat.* **215** (2021) 209 (https://doi.org/10.5004/dwt.2021.26765)
7. B. Isik, F. Cakar, O. Cankurtaran, *Mater. Sci. Eng., B* **293** (2023) 116451 (https://doi.org/10.1016/j.mseb.2023.116451)
8. C. Karaman, O. Karaman, P-L. Show, H. Karimi-Maleh, N. Zare, *Chemosphere* **290** (2022) 133346 (https://doi.org/10.1016/j.chemosphere.2021.133346)
9. S. Daffalla, A. Taha, E. Da'na, M. R. El-Aassar, *Water* **16** (2024) 1449 (https://doi.org/10.3390/w16101449)
10. R. O. Yakubu, M. N. Yaro, S. Habibu, S. Nasir, *ChemSearch J.* **15** (2024) 8 (https://www.ajol.info/index.php/csj/article/view/273584)
11. T. A. Aragaw, F. M. Bogale, *Front. Environ. Sci.* **9** (2021) 764958 (https://doi.org/10.3389/fenvs.2021.764958)
12. A. M. Elgarahy, K. Z. Elwakeel, S. H. Mohammad, G. A. Elshoubaky, *Clean. Eng. Technol.* **4** (2021) 100209 (https://doi.org/10.1016/j.clet.2021.100209)
13. A. P. Ingle, S. Saxena, M. P. Moharil, J. D. Rivaldi, L. Ramos, A. K. Chandel, *Biotechnol. Sustain. Mater.* **2** (2025) 1 (https://doi.org/10.1186/s44316-025-00025-2)
14. B. Knolmajer, I. Jócsák, J. Taller, S. Keszthelyi, G. Kazinczi, *Agronomy* **14** (2024) 497 (https://doi.org/10.3390/agronomy14030497)
15. Environmental Protection Agency, The Ministry of Environmental Protection of the Republic of Serbia, https://sepa.gov.rs/wp-content/uploads/2024/10/Vazduh2023.pdf (date accessed: 09.09.2025)
16. B. Yousaf, G. Liu, Q. Abbas, M. U. Ali, R. Wang, R. Ahmed, C. Wang, M. I. Al-Wabel, A. R. A. Usman, *J. Clean. Prod.* **195** (2018) 458 (https://doi.org/10.1016/j.jclepro.2018.05.246)
17. W. Lian, L. Yang, S. Joseph, W. Shi, R. Bian, J. Zheng, L. Li, S. Shan, G. Pan, *Bioresour. Technol.* **317** (2020) 124011 (https://doi.org/10.1016/j.biortech.2020.124011)
18. D. T. C. Nguyen, H. T. N. Le, T. T. Nguyen, T. T. T. Nguyen, R. K. Liew, L. G. Bach, T. D. Nguyen, D-V. N. Vo, , T. V. Tran, *Sci. Total Environ.* **797** (2021) 149195 (https://doi.org/10.1016/j.scitotenv.2021.149195)
19. N. Nedić, T. Tadić, B. Marković, A. Nastasović, A. Popović, S. Bulatović, *Separations* **11** (2024) 310 (https://doi.org/10.3390/separations11110310)
20. H. D. Bouras, A. RédaYeddou, N. Bouras, A. Chergui, L. Favier, A. Amrane, N. Dizge, *Water Sci. Technol.* **83** (2021) 622 (https://doi.org/10.2166/wst.2021.005)
21. S. Sudarsan, G. Murugesan, T. Varadavenkatesan, R. Vinayagam, R. Selvaraj, *Sci. Rep.* **15** (2025) 1831 (https://doi.org/10.1038/s41598-025-86032-9)
22. R. Lafi, I. Montasser, A. Hafiane, *Adsorption Sci. Technol.* **37** (2019) 160 (https://doi.org/10.1177/0263617418819227)
23. C. Meghana, B. Juhi, N. Rampal, P. Vairavel, *Desalin. Water Treat.* **207** (2020) 373 (https://doi.org/10.5004/dwt.2020.26389)
24. Q. Li, M. Wang, X. Yuan, D. Li, H. Xu, L. Sun, F. Pan, D. Xia, *Environ. Technol.* **42** (2021) 1552 (https://doi.org/10.1080/09593330.2019.1673830)

25. Y. A. Teymur, F. Güzel, *Environ. Sci. Pollut. Res.* **32** (2025) 11251 (https://doi.org/10.1007/s11356-025-36391-7)
26. F. Z. Batana, H. D. Bouras, H. Aouissi, *Egypt. J. Chem.* **65** (2022) 225 (https://doi.org/10.21608/ejchem.2022.113994.5188)
27. M. Stjepanović, N. Velić, A. Galić, I. Kosović, T. Jakovljević, M. Habuda-Stanić, *Water* **13** (2021) 279 (https://doi.org/10.3390/w13030279)
28. N. E.-A. El-Naggar, R. A. Hamouda, M. A. Abuelmagd, S. A. Abdelgalil, *Sci. Rep.* **11** (2021) 14953 (https://doi.org/10.1038/s41598-021-94026-6)
29. U. Aslam, T. Javed, *Water Pract. Technol.* **18** (2023) 1051 (https://doi.org/10.2166/wpt.2023.068)
30. S. Sushma, A. Keshav, M. Ramachandran, *J. Serb. Chem. Soc.* **90** (2025) 529 (https://doi.org/10.2298/JSC240520084S)
31. M. Smiri, F. Guey, H. Chemingui, A. B. Dekhil, , S. Elarbaoui, A. Hafiane, *Eur. J. Adv. Chem. Res.* **1** (2020) (https://doi.org/10.24018/ejchem.2020.1.4.9)
32. K. Manzoor, M. Batool, F. Naz, M. F. Nazar, B. H. Hameed, M. N. Zafar, *Biomass Convers. Biorefin*. **14** (2024) 4511 (https://doi.org/10.1007/s13399-022-02741-5)
33. P. VenkataRao, G. SaiTarun, Ch. Govardhani, B. Manasa, P. Joel Joy, M. Vangalapati, *Mater. Today Proc.* **26** (2020) 3009 (https://doi.org/10.1016/j.matpr.2020.02.626)
34. Z. Y. Velkova, G. K. Kirova, M. S. Stoytcheva, V. K. Gochev, *J. Serb. Chem. Soc.* **83** (2018) 107 (https://doi.org/10.2298/JSC170519093V)
35. S. Noreen, U. Khalid, S. M. Ibrahim, T. Javed, A. Ghani, S. Nazf, M. Iqbal, *J. Mater. Res. Tecnol.* **9** (2020) 5881 (https://doi.org/10.1016/j.jmrt.2020.03.115)
36. A. M. Farhan, G. M. Abu-Taweel, I. R. Sayed, H. A. Rudayni, A. A. Allam, W. Al Zoubi, M. R. Abukhadra, *ACS Omega* **9** (2024) 21204 (https://doi.org/10.1021/acsomega.4c01134)
37. I. Mironyuk, M. Myslin, I. Lapchuk, T. Tatarchuk, O. Olkhovy, *Phys. Chem. Solid State* **22** (2021) 561 (https://doi.org/10.15330/pcss.22.3.561-567)
38. S. H. Abbas, A. M. Ridha, K. H. Rashid, A. A. Khadom, *Int. J. Environ. Sci. Technol.* **20** (2023) 13845 (https://doi.org/10.1007/s13762-023-04986-7)
39. S. Latif, A. Zahid, F. Batool, S. Kanwal, A. Ditta, *Environ. Monit. Assess* **197** (2025) 249 (https://doi.org/10.1007/s10661-025-13673-8)
40. A. Kitemangu, M. R. Vegi, N. M. Malima, *Adsorption Sci. Technol.* **2023** (2023) 1 (https://doi.org/10.1155/2023/4319053)
41. A. Alouache, A. Selatnia, H. E. Sayah, M. Khodja, S. Moussous, N. Daoud, *Int. J. Environ. Sci. Technol.* **19** (2022) 2477 (https://doi.org/10.1007/s13762-021-03313-2)
42. S. Parvin, B. K. Biswas, M. A. Rahman, M. H. Rahman, M. S. Anik, M. R. Uddin, *Chemosphere* **236** (2019) 124326 (https://doi.org/10.1016/j.chemosphere.2019.07.057)
43. European Union (2023), *Regulation (EU) 2023/956 of the european parliament and of the council of 10may 2023 establishing a carbon border adjustment mechanism*, http://data.europa.eu/eli/reg/2023/956/oj (date accessed: 09.09.2025)
44. S. Yeshitila, T. G. Asere, M. Yitbarek, F. Melak, *Int. J. Environ. Res.* **19** (2025) 127 (https://doi.org/10.1007/s41742-025-00800-z).